

Synthesis and characterization of biodegradable polyurethanes with unsaturated carbon bonds based on poly(propylene fumarate)

Bin Hu, Chen Ye, Changyou Gao

MOE Key Laboratory of Macromolecular Synthesis and Functionalization, Department of Polymer Science and Engineering, Zhejiang University, Hangzhou 310027, China

Correspondence to: C. Gao (E-mail: cygao@mail.hz.zj.cn)

ABSTRACT: The segmented polyurethanes synthesized from biodegradable polyesters are very promising and widely applicable because of their excellent physicochemical properties. Poly(propylene fumarate) (PPF), a kind of linear aliphatic unsaturated and biodegradable polyesters, has been well recognized in biomedical applications. Herein novel polyurethanes (PPFUs) were synthesized based on the PPF-diol, diisocyanates such as 1,6-diisocyanatohexane, L-lysine diisocyanate, and dicyclohexylmethane diisocyanate, and chain extenders such as 1,4-butylene glycol and L-lysine methyl ester hydrochloride (Lys-OMe·2HCl). By varying the types of diisocyanates, and chain extenders, and the proportion of hard segments, the PPFUs with tailored properties such as mechanical strength and degradation rate were easily obtained. The synthesized PPFUs had an amorphous structure and slight phase separation with strong hydrogen bonding between the soft segments and the hard segments. The elongation of PPFU elastomers reached over 400% with a slow deformation-recovery ability. The PPFUs were more sensitive to alkaline (5 M, NaOH) hydrolysis than acid (2 M, HCl) and oxidative (30 vol %, H₂O₂) erosion. The tensile strength, deformation-recovery ability, and glass transition temperature of the PPFUs were improved with the increase of hard segment proportion, while the degradation rate was opposite because of the faster degradation of the soft segments. *In vitro* culture of smooth muscle cells in the extractant of the PPFUs or on the PPFUs film surface revealed low cytotoxicity and good cytocompatibility in terms of cell viability, adhesion, and proliferation. © 2015 Wiley Periodicals, Inc. *J. Appl. Polym. Sci.* 2015, 132, 42065.

KEYWORDS: biocompatibility; biodegradable; biomaterials; polyurethanes

Received 24 November 2014; accepted 3 February 2015

DOI: 10.1002/app.42065

INTRODUCTION

The biodegradable polymers play significant roles in many fundamental fields such as agriculture, environmental protection, foodstuff packaging, and medical devices.^{1–4} In the biomedical field, these materials offer tremendous potentials in many promising applications such as drug delivery,⁵ tissue engineering,⁶ regenerative medicine,⁷ gene therapy,⁸ etc. Many of the applications rely on their distinctive biodegradable ability with nontoxic byproducts for organisms, and thereby no special treatment is required to remove the materials, which is of great importance to prevent secondary injury. The biodegradable polymers are generally consisted of natural and synthetic species. The latter offers advantages over the former with versatile and controlled physicochemical properties, without the fear of antigenicity and batch-to-batch variation.⁹ Dating back to the approval of biodegradable sutures in the 1960s,¹⁰ the synthetic biodegradable materials have been developed for over five decades, and a variety of novel materials emerged to settle different problems.

Polyesters, polyethers, polyurethanes, polyanhydrides, and polyaminoacids are the representative synthetic biodegradable polymers.⁹ In particular, the segmented polyurethanes (SPUs) made from biodegradable polyesters and polyethers are intensively investigated in biomedical fields because of their excellent mechanical and processing properties, controllable degradation rate, and adequate biocompatibility.^{10–16} Generally, the biodegradable SPUs (BSPUs) are synthesized from biodegradable macromolecular polyols and aliphatic diisocyanates without mutagenic aromatic degradation products such as 1,6-diisocyanatohexane (HDI), 1,4-diisocyanatobutane (BDI), isophorone diisocyanate (IPDI), L-lysine diisocyanate (LDI), and dicyclohexylmethane diisocyanate (HMDI). When the traditional two-step method is used to synthesize the polyurethanes, low molecular diols and diamines are always adopted during the chain extension process. A variety of BSPUs have been investigated based on the biodegradable polyester and polyether polyols, such as poly(ϵ -caprolactone) (PCL),¹⁷ polycarbonate (PC),¹⁸ poly(L-lactide) (PLA),¹⁹ poly(β -hydroxybutyrate) (PHB),²⁰ etc.

More diverse performance such as mechanical and surface properties can be easily tuned compared to their original polymers used to synthesize the BSPUs.

However, so far most BSPUs have been derived from the saturated macromolecular polyols (PCL, PC, PLA, and PHB), which are lack of reactive sites for modification and functionalization. This is a great drawback, especially when bioactive BSPUs are required. The UV-induced graft polymerization, plasma treatment, and aminolysis are common modification methods but the operation process is a little troublesome and might influence other properties of the material.^{21–23}

Poly(propylene fumarate) (PPF) is a linear aliphatic unsaturated polyester which has been extensively investigated in biomedical applications and used in bone repair and drug delivery fields since 1980s.^{24–27} PPF is mainly synthesized from fumarate acid and propylene glycol which are biocompatible and could be removed out of body by the Krebs cycle.²⁸ Besides, the unsaturated electron deficient double bonds of the fumaric acid units allow further cross-linking or modification of the polymers by methods such as Michael addition reaction.²⁹ The main drawback of PPF is its high viscosity at room temperature, making handling, and processing of the polymer quite cumbersome.³⁰ Most researches about PPF are focused on cross-linking with different reagents such as N-vinyl pyrrolidinone, PPF-diacrylate, diethyl fumarate, and poly(ethylene glycol) dimethacrylate.^{31–33} However, the adjustable ranges of mechanical performance and surface properties such as roughness, hydrophilicity, and surface charge are limited in these cross-linked materials. By proper control over the synthetic process, the PPF can be terminated by hydroxyl groups, and in this case it is suitable for synthesis of unsaturated polyurethanes as the soft segments. The obtained polyurethanes based on PPF (PPFUs) are expected to possess excellent processing ability, improved mechanical property, and feasible functionalization with the combined advantages of PPF and polyurethane. More importantly, the electron deficient double bonds on the PPFUs backbone offers the unique advantage for modification compared to the traditional BSPUs based on saturated polyesters such as PCL, PLA, PHB, etc.

For this purpose, a traditional two-step solution polymerization is adopted for the PPFU synthesis by using the PPF-diol and HDI, LDI, and HMDI. 1,4-Butylene glycol (BDO) and L-lysine methyl ester hydrochloride (Lys-OMe·2HCl) are used as the chain extenders. Thus, a series of PPFUs are synthesized and the relationship between structure and properties is studied. To the best of our knowledge, this is the first report to synthesize the PPF-based polyurethanes (PPFUs), which show good mechanical properties, biodegradability, cytocompatibility, but no cytotoxicity. Further modification of the PPFUs is expectable and is underway.

EXPERIMENTAL

Materials

Fumaric acid (FA), propylene oxide (PO), hydroquinone (HQ), zinc chloride (ZnCl₂), and dibutyltindilaurate (DBTDL) were purchased from Sigma-Aldrich (USA). Diisocyanates such as HDI, LDI, and HMDI were purchased from Alfa Aesar (USA).

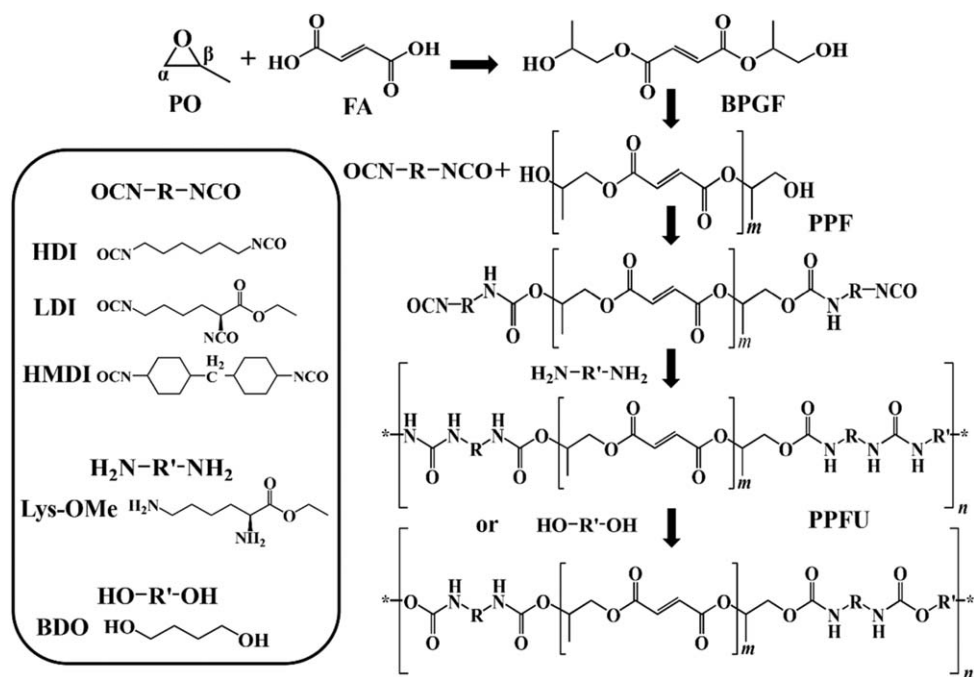
These chemicals were used as received without further purification. Chain extender BDO (TCI, Japan), and L-lysine methyl ester hydrochloride (Lys-OMe·2HCl, TCI, Japan), and all solvents used in the experiment were purified by standard methods. The water used in all experiments was purified via a Millipore Milli-Q purification system and had a resistivity higher than 18.2 MΩ·cm⁻¹.

Synthesis of Polyurethanes

Synthesis of Bis(1,2-Propylene Glycol) Fumarate. Bis(1,2-propylene glycol) fumarate (BPGF) was synthesized according to literature³⁴ with some modifications. Briefly, into a dried three-neck flask 200 mL 4-methyl-2-pentanone, 116 g (1 mol) FA powder and 3 g pyridine were added. The temperature was raised to 85°C with continuous stirring under nitrogen atmosphere, and then 210 mL PO (3 mol) was added dropwise in 3 h. After the mixture was continuously stirred for another 7 h, it was cooled to room temperature. The reaction solution was washed with 300 mL 10% Na₂HPO₄ solution twice and 500 mL 5% KCl solution twice successively. The crude product was dried with anhydrous magnesium sulfate overnight. The remaining solvent was removed by rotary evaporation and further in vacuum oven. The obtained product was viscous pale yellow liquid with a yield about 55%.

Synthesis of PPF. PPF was synthesized from BPGF by a self-transesterification reaction according to the method reported previously.³⁵ Briefly, into a dried three-neck flask 116 g (0.5 mol) BPGF, 0.25 g (2.3×10⁻³ mol) HQ and 1.55 g (1.1×10⁻² mol) ZnCl₂ were added. The temperature was raised to 140°C and maintained for 4 h under negative pressure (<1 mm Hg). The obtained viscous liquid was dissolved in CH₂Cl₂ and washed with 1.85% HCl solution, distilled water, and brine solution successively. The crude product was dried with anhydrous magnesium sulfate overnight and precipitated in ether. The remaining solvent was removed by rotary evaporation. The yield was about 70%.

Synthesis of PPFUs. PPF was dissolved in anhydrous toluene ($\omega \approx 30\%$) and titrated to determine the accurate hydroxyl value according to the ISO 2554-1974 method before polymerization. Based on the hydroxyl value, PPFUs were synthesized in anhydrous dioxane solution by a two-step procedure. In the first stage, PPF was pretreated under vacuum at 110°C for 1 h to remove toluene and trace of water, and then was redissolved in dioxane and mixed in a glass reactor under nitrogen atmosphere with excess mole of diisocyanates in the presence of 0.15 wt % DBTDL in order to form the -NCO terminated prepolymers. In the second stage, chain extender molecules were added to form high molecule weight polyurethanes. The reaction time for the prepolymer formation was 3 h at 70°C, while the chain extending stage lasted for 8 h at 60°C. The obtained polymers were precipitated in ethanol twice and washed with distilled water, and then dried by freeze-drying. The diisocyanates used in this study were HDI, HMDI and LDI, and the chain extenders were BDO and Lys-OMe·2HCl (deprotonation with triethylamine before use). The obtained PPFUs had different chemical compositions and rigid segment contents, as shown in Scheme 1. The



Scheme 1. Synthesis routine of poly(propylene fumarate)-based polyurethanes. PO, propylene oxide; FA, fumaric acid; BPGF, bis(1,2-propylene glycol) fumarate; PPF, poly(propylene fumarate); PPFU, polyurethane based on PPF.

polymer films were prepared by casting solutions on Teflon molds for further characterization.

Physicochemical Characterization of PPFUs

¹H nuclear magnetic resonance (¹HNMR) spectra were recorded on a Bruker DMX500 equipment operated at 500 MHz using CDCl₃ as solvent and tetramethylsilane as reference. Mass spectra were recorded on a Bruker Esquire 3000 plus ion trap mass spectrometer equipped with an electrospray ionization source. Fourier transform infrared (FTIR) spectra were obtained after casting a film on KBr disc on a Vector 22 spectrophotometer (Bruker optics, Switzerland). Ultraviolet visible (UV-vis) absorption spectra were measured on a Shimadzu UV2550 spectrophotometer.

Molecular weights and molecular weight distributions were measured on a Waters 1515 gel permeation chromatography (GPC) setup using poly(methyl methacrylate) standards for calibration. The eluent was THF at 40°C.

The thermal behaviors were evaluated with a MDSC from TA Instruments company (USA) using 8 mg of the polymers. The polymers were heated from room temperature to 200°C and maintained for 2 min to eliminate heat history, and then cooled to -50°C and heated to 200°C again. All procedures were performed under nitrogen atmosphere and the heating or cooling rate was 10°C min⁻¹.

The tensile mechanical properties were measured by an Instron 5540A universal testing machine (USA) with a sample size of 50 × 5 × 0.5 mm and a tensile speed of 100 mm/min. XRD measurements were carried out with a XPERT-PRO diffractometer (Panalytical, Netherlands) using monochromatic radiation (Cu Kα λ = 1.5418 Å) at 35 kV and 24 mA. The samples were regis-

tered in the range 5° < 2θ < 60° with a step count of 10 s and a step size of 0.02° (2θ).

The morphology of the PPFUs was characterized by scanning electron microscopy (SEM, SIRION-100, Netherlands) and transmission electron microscopy (TEM, JEM-1230, USA).

In Vitro Degradation of PPFUs

The *in vitro* degradation was studied in 2M HCl, 5M NaOH and 30 vol % H₂O₂ at 37°C for 15 d, respectively, in order to accelerate the process since degradation of the polymers with a similar PPF structure can last for over 10 months at normal conditions (phosphate buffered saline (PBS), pH 7.4, 37°C).³⁶ The remaining polymers were weighed after degradation to calculate the mass loss.

Cell Culture

Human smooth muscle cells (SMCs) (obtained from Cell Bank of Chinese Academy of Sciences, Shanghai, China) were used to study the cytotoxicity and biocompatibility. The SMCs were cultured at 37°C in a 5% CO₂ humidified environment in Dulbecco's modified eagle medium (DMEM, Gibco, USA) consisting of high-glucose, supplemented with 10% fetal bovine serum (Sijiqing, Hangzhou, China), 100 U/mL penicillin, and 100 μg/mL streptomycin. The medium was changed every 2 d.

For the cytotoxicity assay, the PPFUs films were cut into small pieces (about 2 × 2 mm) and then incubated in the culture medium with a concentration of 0.2 g/mL at 37°C for 24 h to obtain the extractant (ISO 7198-1998). The SMCs were seeded in 96-well plates at a density of 4 × 10³ cells per well, and incubated for 24 h in normal culture medium. The medium was then replaced with the extractant, and the SMCs were continuously cultured for 4 d. At 1, 2 and 4 d, the cytotoxicity was

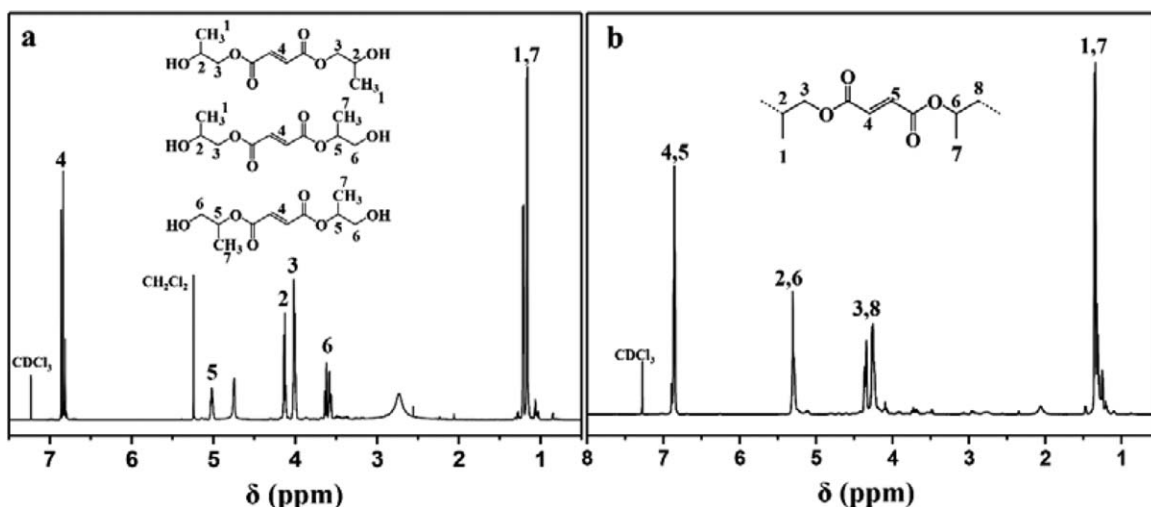


Figure 1. ^1H NMR spectra of (a) BPGF and (b) PPF measured in CDCl_3 .

assayed by 3-(4,5-dimethylthiazol-2-yl)-2,5-diphenyltetrazolium bromide (MTT). Briefly, the cells were incubated in fresh medium containing 0.5 mg/mL MTT for 4 h at 37°C . The dark blue formazan crystals generated by the mitochondria dehydrogenase were dissolved with 100 μL dimethyl sulfoxide, of which 50 μL was transferred into a well of a 96-well plate. The absorbance at 570 nm was measured by a microplate reader (Model 680, BioRad). The data were normalized to the normal medium control group. For the cytocompatibility assay, the PPFUs were dissolved in THF with a concentration of 4%. The solution was cast on the surface of a glass slide which had the same surface area as a 24-well via a spin coater. The SMCs were seeded on the films at a density of 2.5×10^4 cells per well in 1 mL medium, and the cytoviability was assayed and fluorescence images (after FDA staining²³) were captured at 1, 2, and 4 d, respectively.

RESULTS AND DISCUSSION

Synthesis and Characterization of PPF

There are two main methods to synthesize the monomer BPGF: transesterification reaction between diethyl fumarate and propenediol,³⁴ and ring-opening reaction of fumaric acid and propylene oxide.³⁵ The former reaction is usually used to synthesize PPF.^{31–33} However, the latter one has two main advantages: (i) the ring-opening reaction is irreversible and leads to higher reaction extent, and (ii) the impurities such as unreacted fumaric acid and mono-functional products are water-soluble, thus can be easily washed away to ensure the high purity of BPGF. In order to obtain high molecular weight PPFUs, PPF with strict double hydroxyl end groups is mandatory. For these reasons, the latter reaction is more suitable and was adopted for synthesis of BPGF in this study (Scheme 1). By this way the BPGF was successfully synthesized as shown in Figure 1(a).

The resonance peaks in the ^1H NMR spectrum of BPGF [Figure 1(a)] are assigned as follows: δ 1.19 (H1,7, d, 3H, CCH_3), 3.62 (H6, d, 2H, CCH_2OH), 4.03 (H3, d, 1H, OCOCH_2), 4.15 (H2, d, 2H, CHOH), 5.04 (H5, t, 1H, OCOCH), and 6.86 (H4, t, 2H, $\text{CH}=\text{CH}$). The mass spectrum showed the m/z of the synthe-

sized monomer ($\text{C}_{10}\text{H}_{16}\text{O}_6$) was 233.0 (M+H), which is equal to the calculated value. The ^1H NMR and MS results confirmed the successful synthesis of BPGF. According to the reaction mechanism, when fumaric acid was reacted with propylene oxide, three isomers [Figure 1(a)] were obtained because of different ring-opening pathways (site α or site β , Scheme 1). Specifically, proton H2 and H3 are derived from α site ring-opening, whereas H5 and H6 are derived from β site ring-opening. Based on the ^1H NMR integration of these protons (A_{H}), the proportion of α site ring-opening (P_α) was obtained: $P_\alpha = A_{\text{H}2}/(A_{\text{H}2} + A_{\text{H}5}) \approx 63.2\%$, conveying the higher probability of ring-opening on the α site than the β site.

The PPF was synthesized from BPGF through the self-transesterification reaction with ZnCl_2 as catalyst and HQ as inhibitor under 140°C (<1 mm Hg). The resonance peaks in ^1H NMR spectrum [Figure 1(b)] of PPF are assigned as follows: δ 1.34 ppm to the methyl protons, δ 4.28 ppm to the methylene protons, δ 5.30 ppm to the methine protons, and δ 6.85 ppm to the protons on unsaturated double bonds. The ^1H NMR spectrum of PPF exhibited no significant difference to the PPF prepared by two-step transesterification,³⁴ but the titrated hydroxyl value was higher. The molecular weight of the obtained PPF was M_n 1.03 kDa, and M_w 1.52 kDa.

Synthesis and Characterization of PPFUs

A traditional two-step solution polymerization method was used to synthesize PPFUs with different structures from the PPF-diol. By varying the proportion of hard segments, and types of chain extenders and diisocyanates, a series of PPFUs with different physical and chemical properties were synthesized (Scheme 1). Herein, saturated diisocyanates HDI, HMDI and LDI were selected for the PPFUs synthesis considering their non-toxic degradation products. Small molecules such as BDO diol and Lys-OMe-2HCl diamine were used as the chain extenders separately. Meanwhile, by varying the molar ratio of $-\text{OH}/-\text{NCO}$ (1 : 1.1, 1 : 1.3, and 1 : 1.6) in the prepolymers, PPFUs with different proportions of hard segments were prepared. Detail formulation of the PPFUs is summarized in Table I. The PPFUs are designated according to types of diisocyanates, molar

Table I. Formulation and Characterization of the Synthesized PPFUs

Polyurethane type	Diisocyanates	N(-NCO/-OH) ^a	Extender	HS (%) ^b	Mn (kg mol ⁻¹)	PDI ^c	T _g (°C) ^d	T _d (°C)
PPFU/HDI 1.1+Lys-OMe	HDI	1.1 : 1	Lys-OMe	14.5	37.0	4.08	21.8	232.4
PPFU/HDI 1.3+Lys-OMe	HDI	1.3 : 1	Lys-OMe	21.9	25.8	2.61	25.8	279.4
PPFU/HDI 1.6+Lys-OMe	HDI	1.6 : 1	Lys-OMe	29.1	29.2	2.87	33.7	274.2
PPFU/HDI 1.6+BDO	HDI	1.6 : 1	BDO	24.2	31.3	2.95	23.1	273.9
PPFU/HMDI 1.6+Lys-OMe	HMDI	1.6 : 1	Lys-OMe	35.4	27.2	2.65	60.4	276.4
PPFU/LDI 1.6+Lys-OMe	LDI	1.6 : 1	Lys-OMe	34.0	29.1	3.23	40.5	275.3

^aMolar ratio of -NCO and -OH during prepolymerization.

^bHard segment proportion = (weight of diisocyanates + weight of chain extender)/total weight of monomers.

^cPolydispersity index (Mw/Mn) determined by GPC.

^dDetermined according to second heating curves of DSC.

ratios of -NCO/-OH, and types of chain extenders. For example, PPFU/HDI 1.6+Lys-OMe is referred to PPFU whose diisocyanate and chain extender are HDI and Lys-OMe, respectively, and molar ratio of -NCO/-OH is 1.6 : 1 in the prepolymer.

The basic physiochemical properties of the PPFUs such as molecular weight and glass transition temperature (T_g) are summarized in Table I. According to the GPC results (Table I), all the PPFUs had a similar number average molecular weight of 30 kDa with a relatively large polydispersity index. The PPFU/HDI 1.1+Lys-OMe has a larger polydispersity index of about 4. The polycondensation generally results in polymers of larger distribution in Mw compared with other polymerization methods such as radical polymerization. Moreover, the PPF macro-diol used here had an Mn of 1.03 kDa and a comparatively large polydispersity index (about 1.5). Therefore, the PPFUs with a larger proportion of PPF soft segment, for example, the PPFU/HDI 1.1+Lys-OMe, will have a rather larger molecular weight distribution. All the PPFUs had a decomposition temperature (T_d) up to 230°C, revealing good enough thermal stability for processing and biomedical purposes. The hard segment proportions (HS %) of PPFUs were varied from 14.5% to 35.4%, and T_g was changed from 21.8°C to 60.4°C. Basically, improving the HS % would increase the T_g. Meanwhile, the PPFU with a softer chain structure would have a lower T_g. When the diisocyanates were changed from HDI to LDI and HMDI, the T_g apparently increased because HDI has a much more flexible structure than LDI and HMDI. Compared to the PPFU/HDI 1.6+Lys-OMe, the PPFU/HDI 1.6+BDO had a much lower T_g (ΔT ≈ 10°C), which is consistent with their structures: the -NHCOO- has a much weaker hydrogen bonding effect and cohesive energy than the -NHCONH-. For the PPFUs obtained from the same chain extender of Lys-OMe, the PPFU/HDI 1.1+Lys-OMe with a lowest HS % exhibited the lowest T_g of 21.8°C, while the PPFU/HMDI 1.6+Lys-OMe with a highest HS % and hardest chain structure exhibited the highest T_g of 60.4°C. T_g of PPF (Mn = 1160, PDI = 1.42) is about -10°C measured by DSC,³⁰ thus all the PPFUs showed notable increase in T_g.

Figure 2 shows that all the PPFUs had similar absorption peaks in the FITR spectra. The absorbance at 3385, 1725, and 1154 cm⁻¹ are the typical vibrations of hydrogen bonded -NH-,

-C=O, and -O- groups, respectively, indicating the successful synthesis of polyurethanes. Compared to PPF, the vibration of -OH group (3545 cm⁻¹) disappeared in the PPFUs, whereas the vibration of -NH- groups appeared. The existence of absorbance at 1640 cm⁻¹ reveals the maintenance of carbon double bonds in the PPFUs, offering the opportunity for further molecular modification and functionalization. Besides, all the PPFUs were transparent [Figure 3(a)] and had only one obvious absorbance at 210 nm in UV spectra [Figure 3(b)], confirming further the existence of conjugate structure of fumarate acid units. This unique conjugate structure in the PPFUs is of great importance for the carbonyl groups, making the double bond more electron deficiency and easier to react under moderate conditions. From this point of view, the synthesized PPFUs have unique advantage over the traditional saturated polyurethanes.

Mechanical Properties of PPFUs

The mechanical properties of the PPFUs were measured under a tensile speed of 100 mm/min. The representative stress-strain

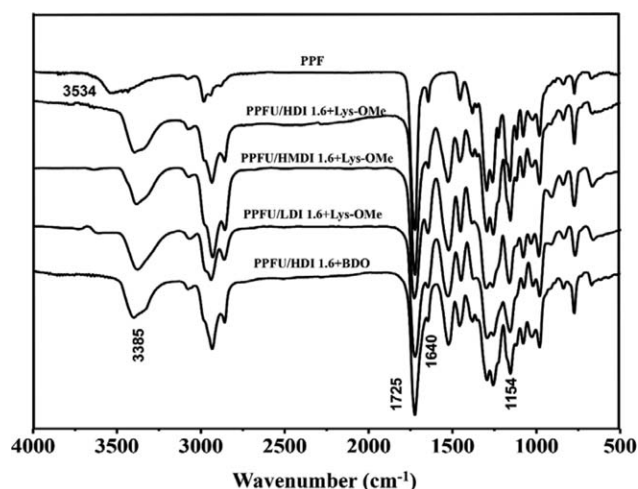


Figure 2. FITR spectra of the synthesized PPFUs. The spectra of PPFU/HDI 1.1+Lys-OMe and PPFU/HDI 1.3+Lys-OMe are not shown since they are almost same as that of the PPFU/HDI 1.6+Lys-OMe. Absorbance at 3385, 1725, 1154, and 1640 cm⁻¹ are typical vibrations of -NH-, -C=O, -O-, and C=C groups, respectively, indicating the successful synthesis of the unsaturated polyurethanes.

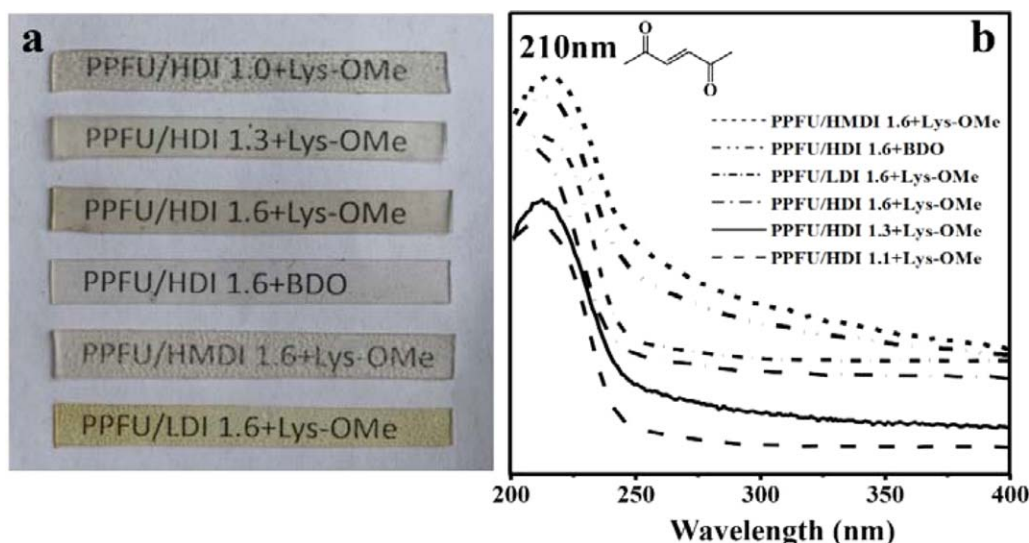


Figure 3. (a) Typical image and (b) UV spectra of PPFUs. All the PPFUs had only one obvious absorbance at 210 nm, indicating the existence of conjugate structure of fumarate acid unit. [Color figure can be viewed in the online issue, which is available at wileyonlinelibrary.com.]

curves are shown in Figure 4, and the detail mechanical parameters including tensile strength (σ_t), tensile modulus (E), and elongation at break (ε) are summarized in Table II. The synthesized PPFUs exhibited maximal tensile strength and modulus of approximate 6 and 70 MPa with large elongation over 400%. The lower tensile strength of PPFUs is mainly attributed to their low Mw,³⁷ and thereby improving the Mw shall be the future focus to improve the mechanical strength of the PPFUs. Moreover, the less degree of microphase separation (see below) should also contribute to some extent because of the easy chain slippage under stress. Since the Tg of PPFUs is higher than

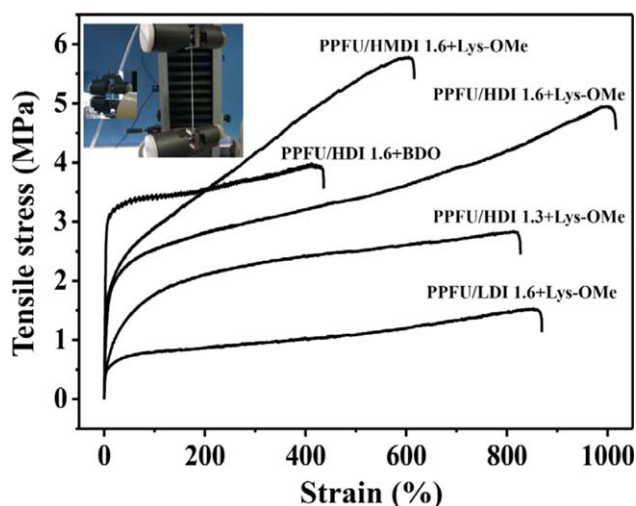


Figure 4. Tensile curves of PPFUs. The curve of PPFU/HDI 1.1+Lys-OMe is not shown because of its critical low tensile strength and over large elongation (over 2000%). The inset image shows the representative large elongation of PPFU/HDI 1.6+Lys-OMe. For this experiment, $50 \times 5 \times 0.5$ mm polymer films were used. Detailed properties are summarized in Table II. [Color figure can be viewed in the online issue, which is available at wileyonlinelibrary.com.]

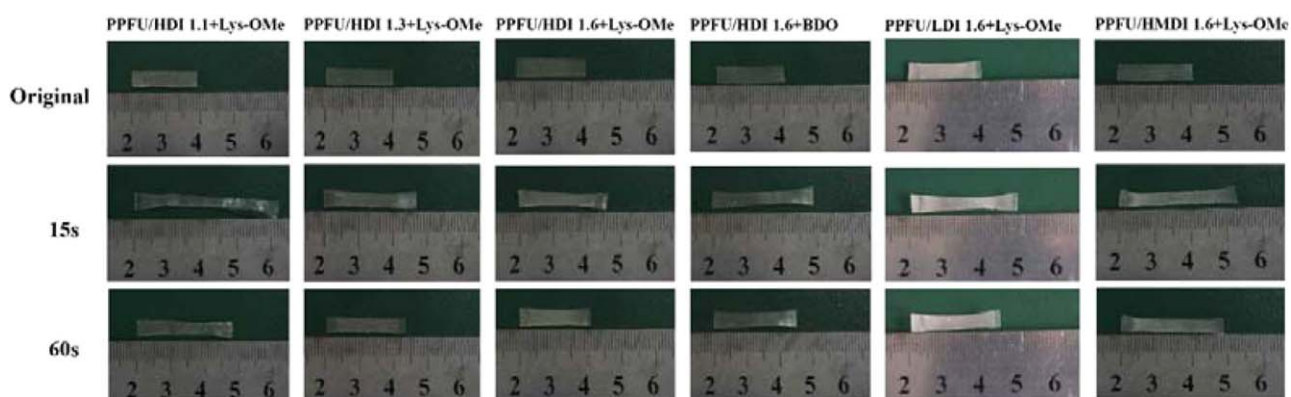
room temperature (except of the PPFU/HDI 1.1+Lys-OMe), Young's modulus is comparatively high when tested under room temperature.

However, the exact values for difference samples are varied greatly. For the series of PPFU/HDI 1.1+Lys-OMe to PPFU/HDI 1.6+Lys-OMe, the tensile strength and modulus increased with the HS % increase. Among all these samples, the PPFU/HDI 1.1+Lys-OMe exhibited weakest strength and largest elongation because of its lowest content of hard segment, and thereby a lowest physical cross-linking degree.³⁸ Besides, the structure of diisocyanates has a decisive role on the corresponding mechanical properties. For example, HMDI has the stiffest structure, and thereby the PPFUs made from HMDI had the highest strength and modulus with the similar feeding ratios of monomers. Moreover, the tensile behavior of PPFUs with different chain extenders also had obvious difference. Compared to the PPFU/HDI 1.6+BDO, the PPFU/HDI 1.6+Lys-OMe showed comparatively superior mechanical properties because of the formation of stronger -NHCONH- structure instead of -COONH- structure.³⁹

The elongation and recovery of the PPFUs was investigated by fixing the polymer strain at 200% elongation for 10 s, and then the length change was measured after load release for 15 and 60 s (Figure 5 and Table II). Briefly, the recovery ability of the PPFUs was improved with the HS % increase, which is consistent with the fact that the hard segments serve as the physical cross-linking units and thereby high HS % is beneficial to the recovery. Indeed, the PPFU/HDI 1.6+Lys-OMe showed the best recovery ability because of its flexible structure and proper hard segment proportion. However, this was not the case when the HS % was critically high especially for the PPFUs made from HMDI. The elasticity of the PPFUs relies on the phase separation of soft and hard segments. At the pretty high proportion of hard segments, the polyurethane would become quite stiff and lack good enough thermo elasticity.³⁹ Therefore, the PPFU/HMDI 1.6+Lys-OMe behaved larger and typical plastic deformation.

Table II. Mechanical Properties of PPFUs

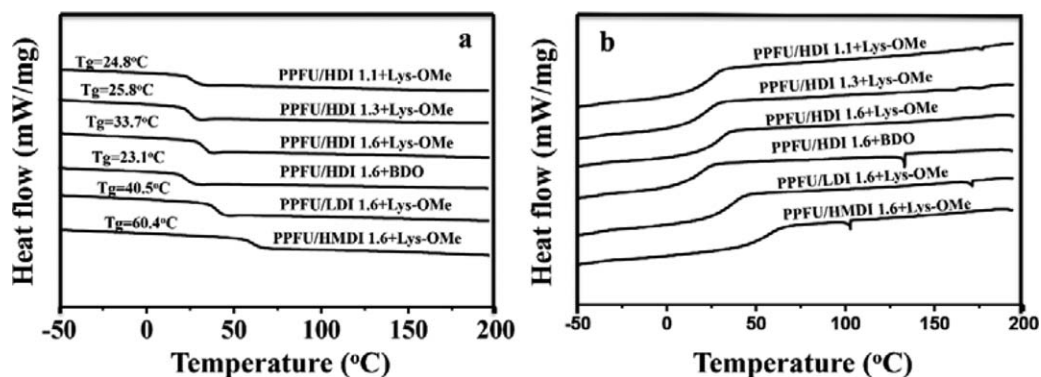
Polyurethane type	σ_t (MPa) ^a	E (MPa) ^b	ϵ_b (%) ^c	ϵ_{15s} (%) ^d	ϵ_{60s} (%) ^e
PPFU/HDI 1.1+Lys-OMe	<1	<5	>1200	110	43
PPFU/HDI 1.3+Lys-OMe	2.7 ± 0.2	25.5 ± 0.8	780 ± 50	35	18
PPFU/HDI 1.6+Lys-OMe	4.9 ± 0.5	42.1 ± 4.7	960 ± 40	28	<5
PPFU/HDI 1.6+BDO	4.3 ± 0.3	93.1 ± 7.7	480 ± 40	42	25
PPFU/LDI 1.6+Lys-OMe	1.3 ± 0.2	29.8 ± 6.6	950 ± 100	40	20
PPFU/HMDI 1.6+Lys-OMe	5.8 ± 0.7	69.4 ± 19.4	640 ± 60	65	40

^a Tensile strength.^b Tensile modulus.^c Elongation at break.^d Elongation after load release for 15 s.^e Elongation after load release for 60 s.**Figure 5.** Digital images of PPFUs before and after elongation and release for different times. The PPFUs were fixed at 200% elongation for 10 s and the length change was measured after load release for 15 and 60 s. [Color figure can be viewed in the online issue, which is available at wileyonlinelibrary.com.]

The high elongation at break, relatively low modulus value, and deformation-recovery ability reveal that the synthesized PPFUs are soft thermoplastic elastomers. By varying the proportion of the hard segments and the chemical structures of diisocyanates and chain extenders, the PPFUs with diverse mechanical properties such as strength and deformation ability could be synthesized for different applications.

Microstructure of PPFUs

The microstructure of polyurethanes determines their properties, which mainly refers to the crystallization and phase separation behaviors. Basically, for the polyurethane elastomers, the crystallization should be avoided under unstressed condition in order to keep the good elasticity, but is favored under stress for self-enhancement.^{40,41} Meanwhile, the thermo elastic PU is

**Figure 6.** DSC curves of PPFUs: (a) heating curves and (b) cooling curves. The heating and cooling rates were 10°C min⁻¹.

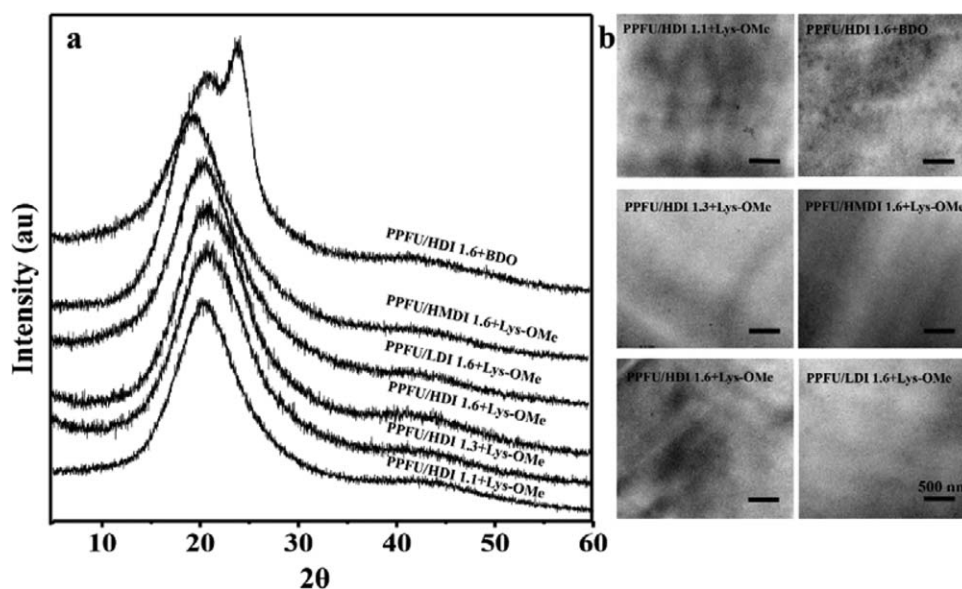


Figure 7. (a) XRD curves and (b) TEM images of PPFUs after osmium tetroxide staining. Scale bar 500 nm.

expected to show microphase separation, which is important for the good elasticity. In summary, the microstructure is decided by the chemical compositions of polyurethanes. In the PPFUs, there are mainly two phases, the soft segments of PPF and the hard segments of diisocyanates and chain extenders, and both phases have the crystallization possibility. PPF is a kind of crystalline polyesters with the crystallinity near 37%.³⁰ However, the XRD results show that all the PPFUs had an amorphous halo with a maximum at $2\theta = 20^\circ$ except of the PPFU/HDI 1.6+BDO, which had a weak peak at 24° on top of this amorphous background [Figure 7(a)]. The microstructure of amorphous PPFUs was further verified by TEM observation [Figure 7(b)]. The phenomenon could be explained that there are lots of hydrogen bonds between the soft segments and hard segments, which largely hinder the crystallization of both parts.⁴² Indeed, the DSC cooling curves [Figure 6(b)] do show small exothermic peaks of crystallization in the PPFU/HDI 1.6+BDO (133°C) and PPFU/HMDI 1.6+Lys-OMe (103°C). This should be attributed to the crystallization of hard segments of high proportion although it is rather weak. Among all the

PPFUs, only the PPFU/HDI 1.6+BDO is totally symmetrical, and thereby has comparatively stronger crystallization ability, but the condition might be quite harsh. The TEM images [Figure 7(b)] show the phase separation with the dark regions as the accumulated soft segments and the white regions as the accumulated hard segments theoretically. It is obvious that the separation degree is rather slight. The possible reason is that the density of ester bonds in PPF is quite higher than that in other macro-diols such as PCL and PHB, and thereby the strong hydrogen interaction between the soft and hard segments increases the miscible degree of both parts.

In summary, the PPFUs are generally in an amorphous state with limited phase separation. Only one glass transition temperature appeared in the DSC curves, revealing the good compatibility of the soft and hard segments, and thereby the lower crystallization and microphase separation. This unique microstructure leads to higher Young's modulus but lower strength. In an ideal thermoplastic elastomer, the microphase separation of the soft and hard segments is complete. The soft part could easily deform but the hard part offers considerable physical

Table III. Mass Loss (%) of PPFUs Under Different Degradation Conditions

Polyurethane type	Mass loss (%) ^a		
	Hydrolysis		Oxidation H ₂ O ₂ (30 vol %)
	HCl (2M)	NaOH (5M)	
PPFU/HDI 1.1+Lys-OMe	8.46 ± 2.56	100	7.38 ± 3.38
PPFU/HDI 1.3+Lys-OMe	6.57 ± 2.13	100	5.35 ± 2.74
PPFU/HDI 1.6+Lys-OMe	4.01 ± 1.37	76.48 ± 10.11	3.99 ± 0.58
PPFU/HDI 1.6+BDO	6.45 ± 0.83	78.64 ± 15.32	4.04 ± 0.94
PPFU/HMDI 1.6+Lys-OMe	4.65 ± 1.29	46.89 ± 6.49	11.42 ± 2.40
PPFU/LDI 1.6+Lys-OMe	10.82 ± 3.76	100	16.30 ± 3.19

^a After being incubated in HCl (2M), NaOH (5M), H₂O₂ (30 vol %) at 37°C for 15 d, respective.

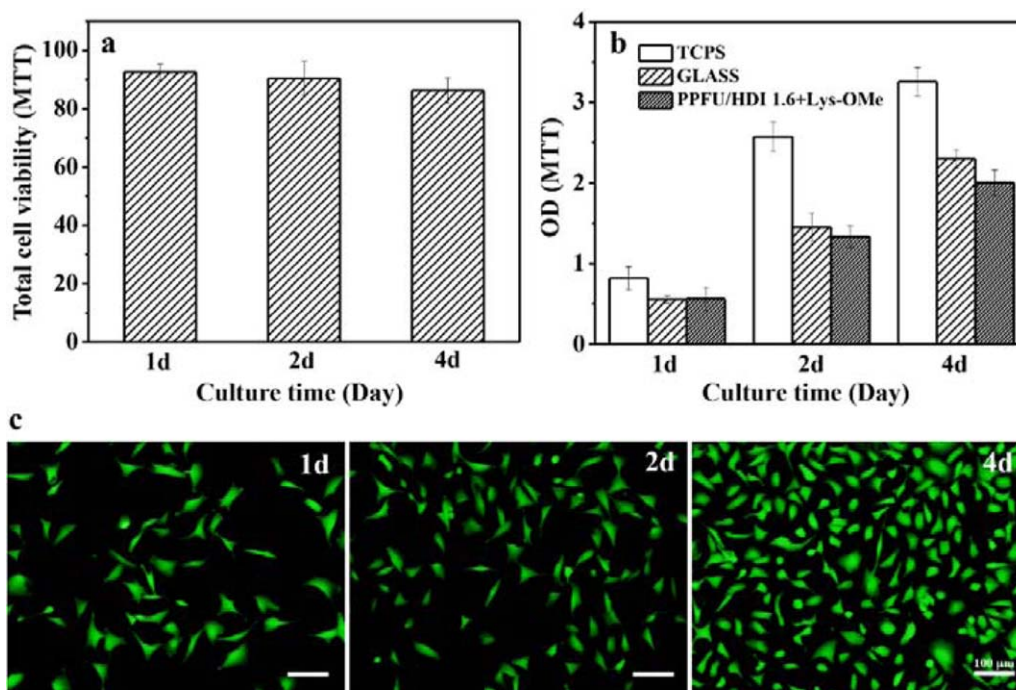


Figure 8. MTT assay of (a) extract of PPFU/HDI 1.6+Lys-OME and (b) viability of SMCs on different surfaces. (c) Fluorescence micrographs of SMCs (stained by FDA before imaging) cultured on PPFU/HDI 1.6+Lys-OME films for different time. Scale bar 100 μm . [Color figure can be viewed in the online issue, which is available at wileyonlinelibrary.com.]

cross-linking units under stress, thus the material would exhibit good mechanical strength and quick deformation recovery speed. The difference in the microstructure of PPFUs can also explain the slow deformation recovery speed of PPFUs.

In Vitro Degradation and Cytocompatibility of PPFUs

The *in vitro* degradation of PPFUs was studied in 2 M HCl, 5 M NaOH and 30 vol % H_2O_2 at 37°C for 15 d to accelerate the degradation process, respectively. In these different degradation conditions, the PPFUs exhibited different mass loss (Table III). Tecoflex[®]SG-80A (Thermedics, USA), a commercial nondegradable polyurethane composed of HMDI, BD, and poly(tetramethylene glycol) (PTMG, $M_n = 2$ kDa) could be used as a comparison. It was reported that the Tecoflex[®] had a mass loss of about 1.66%, 1.48%, 2.16% in 2 M HCl, 5 M NaOH, and 30 vol % H_2O_2 , respectively.³⁶ All the PPFUs showed greater mass loss in these conditions and could be defined as biodegradable materials. Especially, the alkaline hydrolysis (mass loss over 40%) led to an obvious higher mass loss in PPFUs than acidic hydrolysis and oxidative medium. It could be inferred that the PPFUs are more stable under acid and oxidative erosion, while the hydrolysis of ester bonds in the soft segments is the main degradation way.⁴³ Interestingly, in 5 M NaOH, all the PPFUs showed higher mass loss than the soft segment proportion (1-HS %) and some samples (PPFU/HDI 1.1+Lys-OME, PPFU/HDI 1.3+Lys-OME and PPFU/LDI 1.6+Lys-OME) were even degraded completely, demonstrating that the hard segments of PPFUs could be degraded too. Another phenomenon was that the mass loss decreased with the HS % increase because of the faster degradation rate of the soft segments. Besides, the PPFUs

synthesized from LDI exhibited higher mass loss than those from HDI and HMDI because the hard segment structure of LDI is comparatively sensitive to degradation.⁴³ Therefore, by varying the HS % and diisocyanates the degradation rate of the synthesized PPFUs could be controlled for diverse applications such as vascular grafts and heart valves.

To evaluate the cytotoxicity and cytocompatibility of the PPFUs family for possible biomedical applications, the PPFU/HDI 1.6+Lys-OME was selected as a representative to culture with human SMCs. Figure 8(a) shows that the overall cell viability of SMCs measured by MTT assay was over 85%, revealing that the extractant of PPFU/HDI 1.6+Lys-OME did not show obvious cytotoxicity. To compare the cytocompatibility, the SMCs were further cultured on the polymer films, glass, and TCPS, respectively. The increase of OD values [Figure 8(b)] suggest that SMCs could proliferate on all the surfaces. Although the proliferation of SMCs on the PPFU/HDI 1.6+Lys-OME film was not as good as on the TCPS, it was close to that on the glass. The fluorescence micrographs [Figure 8(c)] are consistent with the MTT assay, and further reveal that the SMCs could well attach and proliferate on the PPFUs surface, suggesting the good cytocompatibility. This is very promising and is significantly better than the traditional PUs and other synthetic biopolymers, since generally the synthetic biopolymers are not compatible enough to support cell adhesion and proliferation.⁴⁴

CONCLUSIONS

A series of novel biodegradable SPUs were successfully synthesized with PPF as the soft segments by a two-step

polymerization. By varying the types of diisocyanates and chain extenders, and the proportions of hard segments, the PPFUs have regular structure with tailoring properties such as controllable deformation recovery ability and degradation rate. The obtained amorphous PPFU elastomers exhibited good mechanical properties with slight phase separation and strong hydrogen bonding between the soft segments and the hard segments. The PPFUs were more sensitive to alkaline hydrolysis than to acid and oxidative erosion. Both the soft and hard segments could be degraded in alkaline medium. The tensile strength and recovery ability of the PPFUs were improved with the HS % increase, while the degradation rate was opposite because of the faster degradation rate of the soft segment. Among the diisocyanates used, the PPFUs synthesized from HMDI showed comparatively higher mechanical strength and T_g but slower deformation recovery and degradation rate, while the PPFUs synthesized from HDI and LDI were more flexible and easier to be degraded.

Further optimization of the molecular structures and M_w is necessary to improve the comprehensive properties of the PPFUs. For example, the PPF with a still higher M_w may improve the tensile strength of PPFUs, and copolymerization with other polyethers such as PEG can induce better microphase separation and increase hydrophilicity. Bioactive molecules are easily grafted by reactions such as Michael addition to endow the PPFUs with some specific biological functions. Moreover, the degradation rate of PPFUs can be better manipulated by introducing pH and redox-response units. In summary, as a novel kind of biodegradable elastomers with low cytotoxicity and good cytocompatibility, the PPFUs have promising perspectives as substrates and carriers for tissue engineering, drug delivery, and other biomedical applications.

ACKNOWLEDGMENTS

This study is financially supported by the Natural Science Foundation of China (21434006 and 21374097), and the National Basic Research Program of China (2011CB606203).

REFERENCES

1. Tharanathan, R. N. *Trends Food Sci. Technol.* **2003**, *14*, 71.
2. Gross, R. A.; Kalra, B. *Science* **2002**, *297*, 803.
3. Scarascia-Mugnozza, G.; Schettini, E.; Vox, G.; Malinconico, M.; Immirzi, B.; Pagliara, S. *Polym. Degrad. Stab.* **2006**, *91*, 2801.
4. Tian, H.; Tang, Z.; Zhuang, X.; Chen, X.; Jing, X. *Prog. Polym. Sci.* **2012**, *37*, 237.
5. Nicolas, J.; Mura, S.; Brambilla, D.; Mackiewicz, N.; Couvreur, P. *Chem. Soc. Rev.* **2013**, *42*, 1147.
6. Guo, B.; Ma, P. X. *Sci. Chin. Chem.* **2014**, *57*, 490.
7. Panyam, J.; Labhasetwar, V. *Adv. Drug Deliv. Rev.* **2003**, *55*, 329.
8. Serrano, M. C.; Chung, E. J.; Ameer, G. *Adv. Funct. Mater.* **2010**, *20*, 192.
9. Doppalapudi, S.; Jain, A.; Khan, W.; Domb, A. J. *Polym. Adv. Technol.* **2014**, *25*, 427.
10. Middleton, J. C.; Tipton, A. J. *Biomaterials* **2000**, *21*, 2335.
11. Han, J.; Fei, G.; Li, G.; Xia, H. *Macromol. Chem. Phys.* **2013**, *214*, 1195.
12. Hung, K. C.; Tseng, C. S.; Hsu, S. h. *Adv. Healthc. Mater.* **2014**, *3*, 1578.
13. Karchin, A.; Simonovsky, F. I.; Ratner, B. D.; Sanders, J. E. *Acta Biomater.* **2011**, *7*, 3277.
14. Nelson, D. M.; Baraniak, P. R.; Ma, Z.; Guan, J.; Mason, N. S.; Wagner, W. R. *Pharm. Res.* **2011**, *28*, 1282.
15. Yoshii, T.; Hafeman, A. E.; Esparza, J. M.; Okawa, A.; Gutierrez, G.; Guelcher, S. A. *J. Tissue Eng. Regen. Med.* **2012**, *8*, 589.
16. Song, N.-J.; Jiang, X.; Li, J.-H.; Li, J.-S.; Fu, Q. *Chin. J. Polym. Sci.* **2013**, *31*, 1451.
17. Niu, Y.; Chen, K. C.; He, T.; Yu, W.; Huang, S.; Xu, K. *Biomaterials* **2014**, *35*, 4266.
18. Špirková, M.; Pavličević, J.; Strachota, A.; Poreba, R.; Bera, O.; Kaprálková, L.; Baldrian, J.; Šlouf, M.; Lazić, N.; Budinski-Simendić, J. *Eur. Polym. J.* **2011**, *47*, 959.
19. Wang, W.; Ping, P.; Chen, X.; Jing, X. *Eur. Polym. J.* **2006**, *42*, 1240.
20. Naguib, H. F.; Aziz, M. S. A.; Sherif, S. M.; Saad, G. R. J. *Polym. Res.* **2011**, *18*, 1217.
21. Deng, J.; Wang, L.; Liu, L.; Yang, W. *Prog. Polym. Sci.* **2009**, *34*, 156.
22. Chen, J.-P.; Su, C.-H. *Acta Biomater.* **2011**, *7*, 234.
23. Zhu, Y.; Mao, Z. W.; Gao, C. Y. *Biomacromolecules* **2013**, *14*, 342.
24. Salarian, M.; Xu, W. Z.; Biesinger, M. C.; Charpentier, P. A. *J. Mater. Chem. B* **2014**, *2*, 5145.
25. Lee, J. W.; Kang, K. S.; Lee, S. H.; Kim, J.-Y.; Lee, B.-K.; Cho, D.-W. *Biomaterials* **2011**, *32*, 744.
26. Choi, J.; Kim, K.; Kim, T.; Liu, G.; Bar-Shir, A.; Hyeon, T.; McMahon, M. T.; Bulte, J. W.; Fisher, J. P.; Gilad, A. A. J. *Control. Release* **2011**, *156*, 239.
27. Malachowski, K.; Breger, J.; Kwag, H. R.; Wang, M. O.; Fisher, J. P.; Selaru, F. M.; Gracias, D. H. *Angew. Chem.* **2014**, *126*, 8183.
28. Timmer, M. D.; Ambrose, C. G.; Mikos, A. G. *Biomaterials* **2003**, *24*, 571.
29. Chan, J. W.; Hoyle, C. E.; Lowe, A. B.; Bowman, M. *Macromolecules* **2010**, *43*, 6381.
30. Wang, S. F.; Lu, L. C.; Yaszemski, M. J. *Biomacromolecules* **2006**, *7*, 1976.
31. Ye, C.; Li, Z. H.; Li, D.; Gao, C. Y. *Acta Polym. Sin.* **2012**, *1143*.
32. Lalwani, G.; Henslee, A. M.; Farshid, B.; Parmar, P.; Lin, L.; Qin, Y. -X.; Kasper, F. K.; Mikos, A. G.; Sitharaman, B. *Acta Biomater.* **2013**, *9*, 8365.
33. Cai, L.; Wang, K.; Wang, S. *Biomaterials* **2010**, *31*, 4457.
34. Kasper, F. K.; Tanahashi, K.; Fisher, J. P.; Mikos, A. G. *Nat. Protoc.* **2009**, *4*, 518.

35. Wygant, J. C.; Coeur, C.; Prill, E. J. U.S. Pat. 3,360,546.
36. Chan-Chan, L.; Solis-Correa, R.; Vargas-Coronado, R.; Cervantes-Uc, J.; Cauich-Rodríguez, J.; Quintana, P.; Bartolo-Pérez, P. *Acta Biomater.* **2010**, *6*, 2035.
37. Yoon Jang, J.; Kuk Jhon, Y.; Woo Cheong, I.; Hyun Kim, J. *Colloids Surf. A Physicochem. Eng. Asp.* **2002**, *196*, 135.
38. Lee, B. S.; Chun, B. C.; Chung, Y. -C.; Sul, K. I.; Cho, J. W. *Macromolecules* **2001**, *34*, 6431.
39. Buckley, C.; Prisacariu, C.; Martin, C. *Polymer* **2010**, *51*, 3213.
40. Kanyanta, V.; Ivankovic, A. *J. Mech. Behav. Biomed. Mater.* **2010**, *3*, 51.
41. Rueda-Larraz, L.; d'Arlas, B. F.; Tercjak, A.; Ribes, A.; Mondragon, I.; Eceizaa, A. *Eur. Polym. J.* **2009**, *45*, 2096.
42. Fernandez, C. E.; Bermudez, M.; Versteegen, R. M.; Meijer, E. W.; Muller, A. J.; Munoz-Guerra, S. *J. Polym. Sci. B Polym. Phys.* **2009**, *47*, 1368.
43. Santerre, J. P.; Woodhouse, K.; Laroche, G.; Labow, R. S. *Biomaterials* **2005**, *26*, 7457.
44. Pariente, J. L.; Kim, B. S.; Atala, A. *J. Biomed. Mater. Res.* **2001**, *55*, 33.